Modelling of Turbulent Flow and Mass Transfer with Wall Function and Low-Reynolds Number Closures

S. NEŠIĆ[1], G. ADAMOPOULOS[1], J. POSTLETHWAITE[1] and D. J. BERGSTROM[2]*

Departments of [1]Chemical Engineering and [2]Mechanical Engineering, University of Saskatchewan, Saskatoon, SK S7N 0W0

A recent laser doppler anemometer study, by other researchers, of turbulent flow through a sudden expansion has been simulated using a kinetic energy of turbulence-dissipation rate of turbulence ($k - \epsilon$) model. The near wall region was modelled in two different ways; using wall functions (WF), and a low-Reynolds number (LRN) formulation.

The reattachment length under particular flow conditions was obtained. Radial profiles for the mean axial and radial velocity, turbulence kinetic energy and Reynolds shear stress were determined for six locations downstream of the sudden expansion. Both models performed reasonably well in predicting the flow with the LRN approach performing slightly better than the WF approach near to the wall.

The application of the LRN approach to the calculation of local mass transfer rates in wall bounded complex turbulent flows is demonstrated.

Une étude des écoulements turbulents dans une expansion soudaine par anémométrie laser Doppler a été récemment publiée. Nous avons simulé le problème en utilisant l'énergie cinétique de turbulence-dissipation du modèle de turbulence ($k - \epsilon$). La région proche de la paroi a été modélisée de deux manières différentes: par les fonctions de paroi (WF) et par une formulation à faibles nombres de Reynolds (LRN).

La longueur de rattachement a été obtenue dans des conditions d'écoulement particulières. Nous avons déterminé la distribution radiale de la vitesse axiale et radiale moyenne, l'énergie cinétique turbulente et la contrainte de cisaillement de Reynolds en six points situés en aval de l'expansion soudaine. Les deux modèles se sont relativement bien comportés pour prédire l'écoulement, la méthode LRN s'étant révélée légèrement plus efficace que la méthode WF près de la paroi.

On démontre l'application de la méthode LRN au calcul des vitesses de transfert de matière local dans des écoulements turbulents complexes confinés.

Keywords: turbulence models, low Reynolds number closure, wall mass transfer.

The modelling of erosion–corrosion in complex turbulent flows requires an ability to determine the flow field and local wall mass transfer rates of corrosion reactants and products. In the present study the mass and momentum equations were closed using a kinetic energy of turbulence-dissipation of turbulence energy ($k - \epsilon$) model, which solves two additional transport equations to obtain the local eddy viscosity. The $k - \epsilon$ model closure is superior to the mixing-length models for flows where it is desirable to predict at least some of the characteristics of the turbulent field. At the same time, the relative simplicity of a $k - \epsilon$ model compared to second moment closures makes it a more efficient approach for many industrial applications.

In a recent erosion–corrosion modelling study (Nešić and Postlethwaite, 1991) electrochemically determined local mass transfer results (Sydberger and Lotz, 1982) for a sudden pipe expansion, were correlated with the near-wall (2 mm) turbulent velocity fluctuations predicted by the application of a $k - \epsilon$ model using wall functions (WF). The correlation, which was obtained for a specific geometry, lacked generality and a more fundamental approach is required.

At the high Schmidt numbers encountered in wall mass transfer the small amount of turbulence in the viscous sublayer, which is unimportant from a hydrodynamic standpoint, has a major effect on the rate of mass transfer. Consequently the mass transfer boundary layer is deeply embedded within the viscous sublayer. The WF approach bridges over the viscous sublayer with a universal velocity profile; the first computational node is placed in the logarithmic law region ($30 < y^+ < 150$). An approach was required that extends the validity of the $k - \epsilon$ model to the wall and provides information on the effect of turbulent mass transport within the viscous sub-layer. One such approach is to apply a low-Reynolds-number (LRN) $k - \epsilon$ closure.

Patel et al. (1985) presented a comprehensive review of seven different LRN models and found that only three models, including the model of Lam and Bremhorst (1981), were moderately successful in reproducing experimental data for flows dominated by proximity to the wall. The Lam and Bremhorst (1981) model, which was selected for the present study, is more appealing from a physical point of view than the other two models since it operates with the dissipation rate, ϵ, itself rather than with a dissipation variable selected for the purpose of computational convenience. More recently, others including Nagano and Tagawa (1990) have proposed improved LRN models. These models are essentially similar to that of Lam and Bremhorst (1981) except for the specific choice of the damping functions.

Flow through a sudden expansion was chosen as a generic test case (Nešić, 1991), to study the relationship between the hydrodynamic parameters of the flow and mass transfer controlled erosion–corrosion in disturbed flow conditions. This geometry, extensively studied in fluid dynamics, has a high level of hydrodynamic complexity with separation, reattachment and associated recirculation of the flow, which in turn have a significant effect on a large number of heat and mass transfer devices and processes.

The present paper presents a simulation of the laser doppler anemometer (LDA) results of Steiglmeier et al. (1989) for flow through a sudden expansion, Figure 1, using the WF and LRN approaches near the wall. The application of the LRN approach for the calculation of mass transfer rates under separated flow conditions is also illustrated.

*To whom correspondence should be addressed.

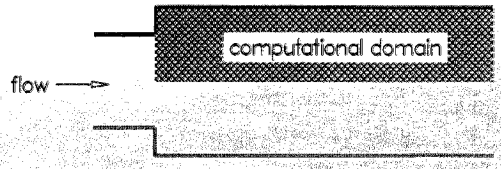

Figure 1 — Flow geometry and computational domain.

The model

The present model is based on a standard single phase $k-\epsilon$ model of turbulence proposed by Launder and Spalding (1972). The conservation equations for the mass, momentum, kinetic energy of turbulence and its dissipation for axisymmetric flow are:

Continuity equation

$$\partial(\rho U)/\partial x + (1/r)\partial(r\rho V)/\partial r = 0 \quad \ldots\ldots (1)$$

Momentum equation in axial direction

$$\partial(\rho U^2)/\partial x + (1/r)\partial(r\rho UV)/\partial r = 2\partial(\mu_{eff}\partial U/\partial x)/\partial x + (1/r)\partial(r\mu_{eff}\partial U/\partial r)/\partial r + (1/r)\partial(r\mu_{eff}\partial V/\partial x)/\partial r - \partial P/\partial x \quad \ldots\ldots (2)$$

Momentum equation in radial direction

$$\partial(\rho UV)/\partial x + (1/r)\partial(r\rho V^2)/\partial r = \partial(\mu_{eff}\partial V/\partial x)/\partial x + (2/r)\partial(r\mu_{eff}\partial V/\partial r)/\partial r + \partial(\mu_{eff}\partial U/\partial r)/\partial x - 2\,\mu_{eff}V/r^2 - \partial P/\partial r \quad \ldots\ldots (3)$$

In Equations (2) and (3), the Boussinesq assumption (Hinze, 1975) has been used for modelling the Reynolds stress. The resultant eddy viscosity model relation is given by:

$$-\overline{\rho u_i u_j} = \mu_t\,[(\partial U_i/\partial x_j) + (\partial U_j/\partial x_i)] - 2\rho k\delta_{ij}/3 \quad (4)$$

where μ_t is defined as the "turbulent viscosity":

$$\mu_t = C_\mu f_\mu(\rho k^2/\epsilon) \quad \ldots\ldots (5)$$

and the kinetic energy of turbulence k and it's dissipation rate ϵ are:

$$k = (\overline{u^2} + \overline{v^2} + \overline{w^2})/2, \qquad \epsilon = \nu\overline{(\partial u_i/\partial x_j)^2} \quad \ldots\ldots (6)$$

Equation for turbulence kinetic energy

$$\partial(\rho Uk)/\partial x + (1/r)\partial(r\rho Vk)/\partial r = \partial[(\mu_{eff}/\sigma_k)(\partial k/\partial x)]/\partial x + [1/r]\,\partial[(r\mu_{eff}/\sigma_k)(\partial k/\partial r)]/\partial r + G_k - \rho\epsilon \quad \ldots (7)$$

Equation for dissipation of kinetic energy of turbulence

$$\partial(\rho U\epsilon)/\partial x + (1/r)\partial(r\rho V\epsilon)/\partial r = \partial[(\mu_{eff}/\sigma_\epsilon)(\partial\epsilon/\partial x)]/\partial x + [1/r]\,\partial[(r\mu_{eff}/\sigma_\epsilon)(\partial\epsilon/\partial r)]/\partial r + (\epsilon/k)(C_{\epsilon 1} f_1 G_k - C_{\epsilon 2} f_2 \rho\epsilon) \quad \ldots\ldots (8)$$

In Equations (7) and (8) the generation of kinetic energy of turbulence G_k is:

$$G_k = \mu_{eff}\{2[(\partial U/\partial x)^2 + (\partial V/\partial r)^2 + (V/r)^2] + [(\partial U/\partial r) + (\partial V/\partial x)]^2\} \quad \ldots\ldots (9)$$

The effective viscosity μ_{eff} is:

$$\underbrace{\mu_{eff}}_{\text{effective}} = \underbrace{\mu}_{\text{molecular}} + \underbrace{\mu_t}_{\text{turbulent}} \quad \ldots\ldots (10)$$

The standard model constants (Patel et al., 1985) are used in the above equations

$$C_\mu = 0.09,\ C_{\epsilon 1} = 1.44,\ C_{\epsilon 2} = 1.92,\ \sigma_k = 1.0,\ \sigma_\epsilon = 1.3$$

Boundary conditions

Since the above set of partial differential Equations (2), (3), (7) and (8) is elliptic it is necessary to define boundary conditions for all variables on all boundaries of the flow domain: inlet, exit, walls and symmetry axis. At the inlet, the profile of the mean axial velocity was obtained from the experimental results of Stieglmeier et al. (1989). The turbulent parameters were expressed via the turbulence intensity ($T_u = \bar{u}/U$). Thus for the turbulence inlet boundary condition we can convert T_u data into the k and ϵ values by assuming the length scale L_ϵ, equal to the inlet diameter, and writing:

$$k = (3/2)T_u^2 U^2, \qquad \epsilon = C_\mu^{0.75} k^{1.5}/L_\epsilon \quad \ldots\ldots (11)$$

In the case of axisymmetric flow, $V = 0$ and $\partial\Phi/\partial r = 0$ on the axis. At the exit of the computation domain fully developed flow is assumed. Near the wall two basic approaches are used: the universal wall function (WF) model and the Low Reynolds Number (LRN) model (Lam and Bremhorst, 1985).

The WF approach bridges over the near-wall region with a universal logarithmic velocity profile. The equation for the mean velocity U_c at the first interior node becomes:

$$U^+ = (1/\kappa)\ln(Ey_c^+) \quad \ldots\ldots (12)$$

where

$$U^+ = U_c/U_\tau, \qquad U_\tau = (\tau_w/\rho)^{0.5} \quad \ldots\ldots (13)$$

and typically the first node is located so that

$$30 < y^+ = y_c U_\tau/\nu < 150$$

The kinetic energy of turbulence k and its dissipation ϵ can be obtained from the local equilibrium assumption, i.e. production of turbulence = dissipation. It can be shown that the value of k and ϵ at the first interior node become:

$$k_c = \tau_w/\rho C_\mu^{0.5} \quad \ldots\ldots (14)$$

$$\epsilon_c = C_\mu^{0.75} k_c^{1.5}/\kappa y_c \quad \ldots\ldots (15)$$

The constants used for the logarithmic boundary layer velocity profile are:

$$\kappa = 0.43, \qquad E = 9.5$$

The WF approach, although less demanding than the LRN model, from the aspects of required memory and CPU time, is known to perform worse than the LRN approach for recirculating flows (Yap, 1987). The "universal" velocity profile determined for simple near-wall shear flows, which is employed in the WF approach, is inappropriate when flow separation or reversal is present, and more importantly for mass transfer studies where it is necessary to perform calculations very close to the wall, with "nodes" deeply embedded in the viscous sublayer. A LRN approach, which enables the application of the $k - \epsilon$ turbulence model very close to the wall can give the characteristics of the flow with more accuracy in this region. The main idea behind the LRN approach is to solve the $k - \epsilon$ equations throughout the flow field, including the near-wall region, and then modify the turbulence level in the near-wall region by modifying the turbulent viscosity and dissipation. This modification is done by using correction factors, here called "damping functions", which gradually suppress the turbulence level as the wall is approached.

As discussed in the introduction, the model of Lam and Bremhorst (1985) was selected for this study since it has been used successfully in other flow studies. In the model of Lam and Bremhorst (1985) the damping functions, which are responsible for the modification of the turbulence field in the near-wall region, are given by:

$$f_\mu = [1 - \exp(-0.0165Re_y)]^2 \, [1 + (20.5/Re_T)]$$

$$f_1 = 1 + (0.05/f_\mu)^3$$

$$f_2 = 1 - \exp(-Re_T^2)$$

where $Re_y = yk^{0.5}/\nu$ and $Re_T = k^2/\nu\epsilon$.
At the wall, the boundary conditions for k and ϵ (Patel et al., 1985) are:

$$k = 0, \qquad \partial\epsilon/\partial r = 0$$

Numerical procedure

The conservation equations for mass, axial and radial momentum, kinetic energy of turbulence and its dissipation rate, were solved numerically using the SIMPLE algorithm, of Patankar and Spalding (1972). Non-uniform staggered grids were used with the majority of nodes concentrated in the near-wall region where the gradients of velocity and concentration were the largest. The number of control volumes, as well as the geometrical and flow parameters are given in Table 1. As the number of iterations and the dimensions of the grid indicate, the LRN approach requires significantly greater CPU time and memory storage space than the WF approach. The criterion for convergence was that the total normalized residual be less than 0.001. For purely hydrodynamic LRN models it is usually adequate to place the first node adjacent to the wall at ($y^+ \leq 5$) within in the viscous sublayer.

Results and discussion

The recent results of Stieglmeier et al. (1989) were selected for simulation. They reported detailed radial profiles for axial, radial, and tangential mean velocity, as well as the normal and shear turbulent stresses, and the reattachment length. The profiles were shown for six locations downstream of the sudden expansion and measurements were taken as close as 1 mm for the wall. Their results are especially useful for validation of computational models since measurements were obtained for the Reynolds stress profiles as well as the mean velocity. Stieglmeier et al. (1989) overcame the experimental difficulties encountered by previous investigators relating to the refraction of the laser beams on the cylindrical surfaces of the test section. The difficulty was overcome by fully matching the refractive index of the working fluid with that of the containment glass. A complete summary of uncertainty errors both fixed and variable, was presented in the above paper.

TABLE 1
Test Conditions

Density	863.5 kg/m^3
Kinematic viscosity	6.3×10^{-6} m^2/s
Inlet diameter	50.0 mm
Outlet diameter	80.0 mm
Inlet maximum axial velocity	2.51 m/s
Outlet maximum axial velocity	0.98 m/s
Inlet bulk axial velocity	1.962 m/s
Outlet bulk axial velocity	0.767 m/s
Inlet Reynolds number	1.56×10^4
Outlet Reynolds number	9.75×10^3
WF grid	52×24
Number of iterations for WF	236
LRN grid	93×80
Number of iterations for LRN	2659

Simulations were done by using first the WF model and then the LRN model for the boundary conditions. This was done to assess the benefits of the LRN number model over the WF model since the LRN model requires more computational time and memory for the same flow geometry.

The measured reattachment length ($x_r/D \approx 1.75$) was closely predicted by the LRN and underpredicted by the WF model ($x_r/D \approx 1.18$). The calculation of the reattachment point has been done by estimating the position in the x direction where the axial velocity 1 mm away from the wall changes sign.

The profiles of mean axial velocity are shown in Figure 2. It is clear that both models performed reasonably well. The LRN model gave somewhat better results in the near-wall region especially in the recirculation zone at $x/D = 0.5$ before the reattachment point. This could be anticipated as the universal velocity profile used in WF functions cannot be expected to be valid near the reattachment point. On the other hand in the redeveloped flow region ($x/D = 2.5$) near the centreline the WF performed slightly better. Over most of the profile the discrepancy between the predictions and the measurements was less than 5% which is within the maximum overall error of measurement as reported by Stieglmeier et al. (1989). As might be expected there is a greater discrepancy near the wall, due to the low velocities involved, which result in greater experimental error.

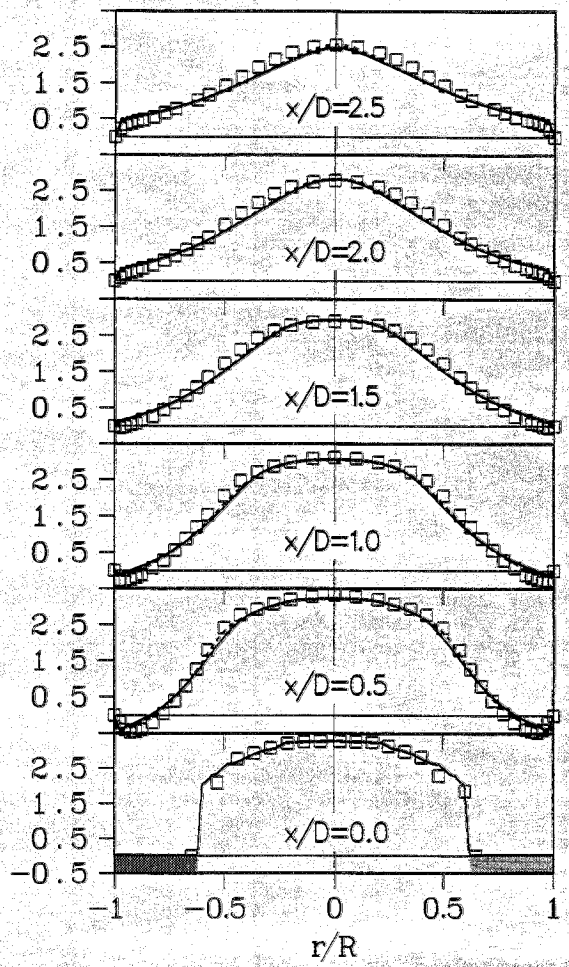

Figure 2 — Radial profiles on mean axial velocity for flow through a sudden expansion; d_{in} = 50.0 mm; d_{out} = 80.0 mm; v_{in} = 2.51 m/s; v_{out} = 0.98 m/s; $Re_{in} = 1.56 \times 10^4$
--- $k - \epsilon$, LRN predictions
____ $k - \epsilon$, WF predictions
□ Stieglmeier et al. (1989) measurements.

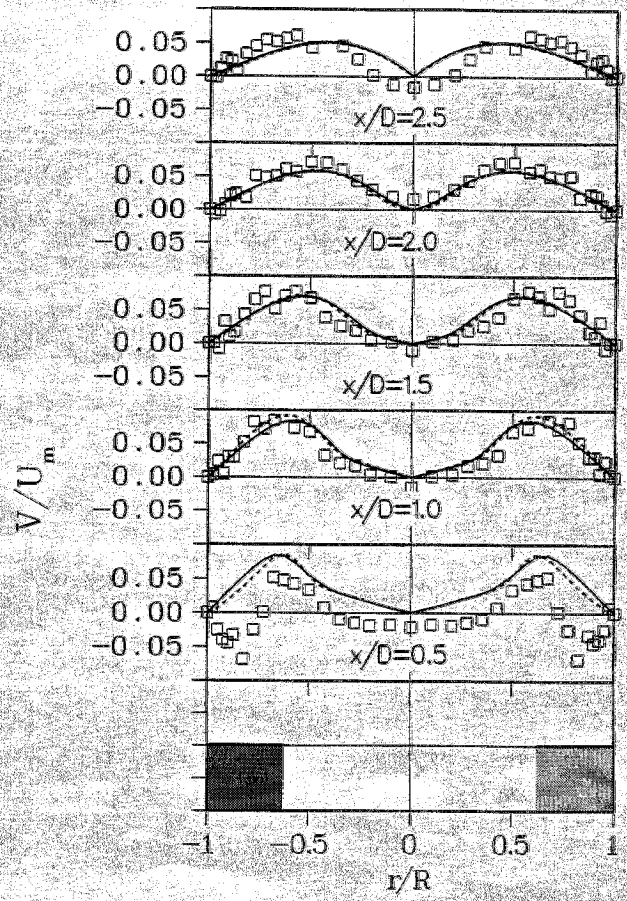

Figure 3 — Radial profiles of mean radial velocity for flow through a sudden expansion; d_{in} = 50.0 mm; d_{out} = 80.0 mm; v_{in} = 2.51 m/s; v_{out} = 0.98 m/s; $Re_{in} = 1.56 \times 10^4$
--- $k - \epsilon$, LRN predictions
____ $k - \epsilon$, WF predictions
□ Stieglmeier et al. (1989) measurements.

The radial velocity profiles are shown in Figure 3. The LRN model performed consistently better than the WF model although the discrepancy between the predictions and measurements was larger than for the axial velocity. This is particularly obvious in the profile at $x/D = 0.5$. This is to be expected since the model underpredicts the location of the reattachment point. The predicted velocities are consistently higher than the measurements and there are no negative values. The existence of negative radial velocities in the experimental data could indicate a very slight tilt of the axis of the measurement system to the flow. Problems in predicting the radial velocity profiles especially in the recirculation region were encountered by other researchers (Zeisel and Durst, 1990; Durret et al., 1988) and this is probably related to inadequate modelling of turbulent transport in this region. Apart from the first profile ($x/D = 0.5$) it can be concluded that the inaccuracy of the predictions was not much larger then the scattering of the measured values for radial velocity.

The model predictions for the kinetic energy of turbulence, k, are given in Figure 4. Stieglmeier et al. (1989) measured all three components of the normal turbulent stress ($\overline{u}^2$, $\overline{v}^2$, $\overline{w}^2$). For comparison purposes the measured values of normal turbulent stresses were summed to give an experimental profile for k. The LRN model was significantly better in the near-wall region of the recirculation region (x/D =0.5). In the near wall region the WF model predicted twice the measured value of k while the LRN model overpredicted turbulence by some 30–50%. This is to be expected since the $k - \epsilon$ model assumes isotropic normal stresses. Further, downstream both models were within 10% of the measured values.

Stieglmeier et al. (1989) measured the turbulent shear stress components associated with the correlation of the velocities fluctuations $\overline{uv}$ and $\overline{uw}$. In the $k - \epsilon$ model the turbulent shear stresses are evaluated through the modified Boussinesq approximation (Hinze, 1975). The turbulent shear stress profiles used by the $k - \epsilon$ model are shown in Figure 5. They indicate some discrepancy with the measured values. Both of the models underpredicted the shear stress near the wall except in the region of the recirculation zone ($x/D = 0.5$) where they slightly overpredicted. In this region the LRN model gives predictions closer to the experimental results than the WF model. Further downstream, the models still describe peak shapes accurately however numerical agreement with experimental results is rather modest. This may be due to the fact that in this region the flow is not fully developed.

Application to wall mass transfer

The $k - \epsilon$, LRN model has been applied to the determination of local wall-mass-transfer rates, elsewhere (Nesić,

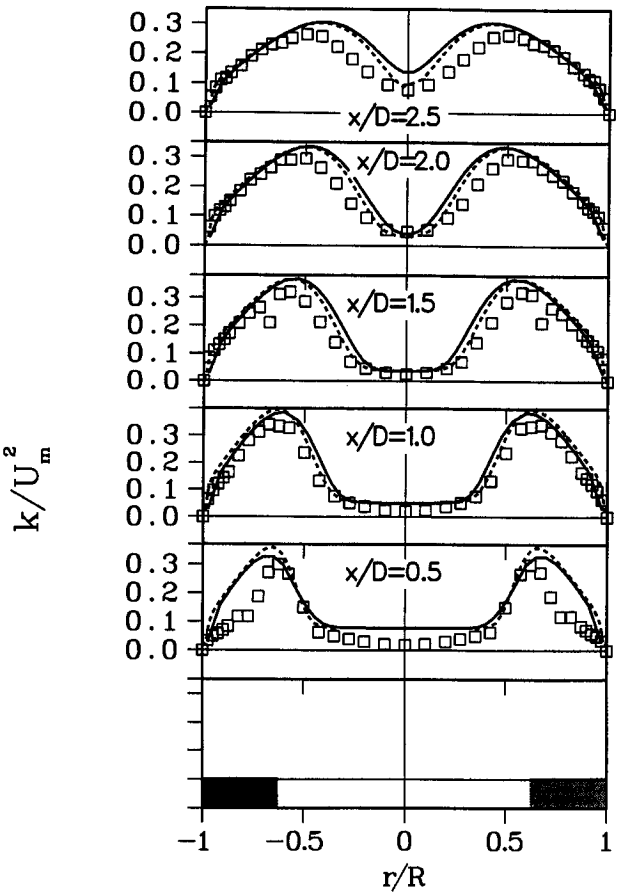

Figure 4 — Radial profiles of kinetic energy of turbulence for flow through a sudden expansion; d_{in} = 50.0 mm; d_{out} = 80.0 mm; v_{in} = 2.51 m/s; v_{out} = 0.98 m/s; $Re_{in} = 1.56 \times 10^4$
--- $k - \epsilon$, LRN predictions
____ $k - \epsilon$, WF predictions
□ Stieglmeier et al. (1989) measurements.

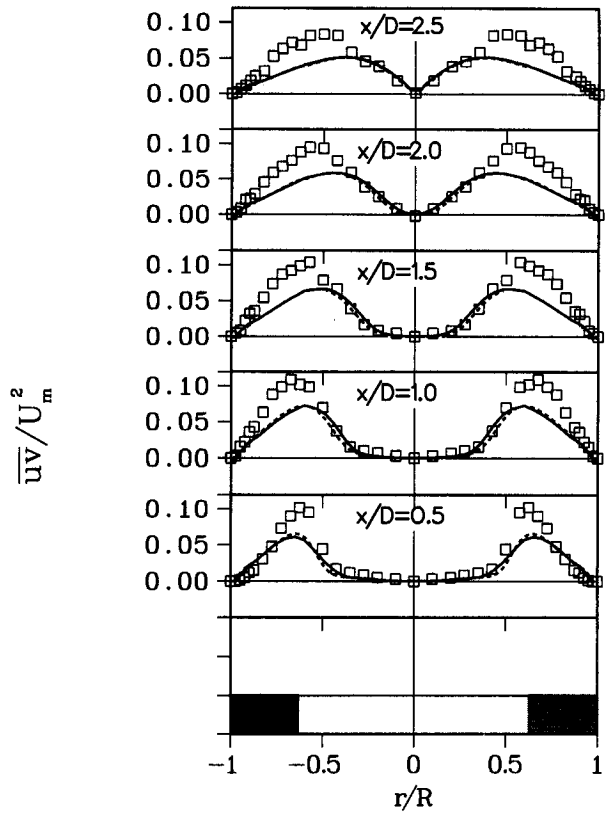

Figure 5 — Radial profiles of turbulent shear stress for flow through a sudden expansion; d_{in} = 50.0 mm; d_{out} = 80.0 mm; v_{in} = 2.51 m/s; v_{out} = 0.98 m/s; $Re_{in} = 1.56 \times 10^4$
--- $k - \epsilon$, LRN predictions
____ $k - \epsilon$, WF predictions
□ Stieglmeier et al. (1989) measurements.

1991; Nešić et al., 1991) and good agreement between predictions and the experimental results of others was obtained. This latter treatment of wall mass transfer solves the mass transport equation simultaneously with the flow equations by assuming an analogy in the mechanisms of turbulent momentum and mass transport. The mass transport equation for a specific species written in an axisymmetric coordinate system is

$$\partial(\rho U M^s)/\partial x + (1/r)\partial(r\rho V M^s)/\partial r = \partial(D^s_{eff}\,\partial M^s/\partial x)/\partial x + (1/r)\partial(rD^s_{eff}\,\partial M^s/\partial r)/\partial r \quad \ldots\ldots\ldots\ldots\ldots (16)$$

where the effective diffusivity is given by:

$$D_{eff} = \mu/\rho Sc + \mu_t/\rho\sigma_m \quad \ldots\ldots\ldots\ldots\ldots (17)$$

effective *molecular* *turbulent*

The value of the turbulent Schmidt number σ_m = 0.9, which is of special importance in mass transfer studies, is according to Kays et al. (1980), constant throughout the bulk of the fluid, especially for fluids with high molecular Schmidt numbers. Measurements have indicated that very close to the wall within the viscous sublayer, the value of σ_m approximately doubles, and following Kays et al. (1980) a value of 1.7 was used in the present study in this region.

The solution of the species mass transport equations gives the concentration field of the species under consideration; dissolved oxygen for example. The local mass transfer rate of the species is determined from a knowledge of the diffusion coefficient and the species concentration at the node closest to the wall. Limiting conditions are assumed, that is the wall concentration is set at zero, and the sole mode of transport between the node closest to the wall and the wall is assumed to be molecular diffusion. The mass transfer coefficient, K, is then calculated using the local mass transfer rate and the overall concentration difference between the bulk solution and the wall.

For purely hydrodynamic LRN models it is usually adequate to place the first node adjacent to the wall somewhere in the viscous sublayer ($y^+ \leq 5$). However, in the case of mass transfer at high molecular Schmidt numbers ($Sc \simeq 1000$), the thickness of the diffusion mass transfer boundary layer is approximately one tenth the viscous sublayer. Therefore, the first node was placed at $y^+ \simeq 0.1$. The final solution fields have shown that only at these distances from the wall does the level of turbulent transport of mass become negligible compared to the molecular diffusional component.

An extension of previously reported wall mass transfer calculations for a ferri-ferro cyanide system at a sudden expansion (Nešić et al., 1991) is shown in Figure 6. In the present paper the calculated rates of mass transfer to small localized areas of the surface are compared to the previously calculated rates of mass transfer with the whole surface area active. Mass transfer to localized areas of the metal surface arises in erosion–corrosion where small areas of protective films

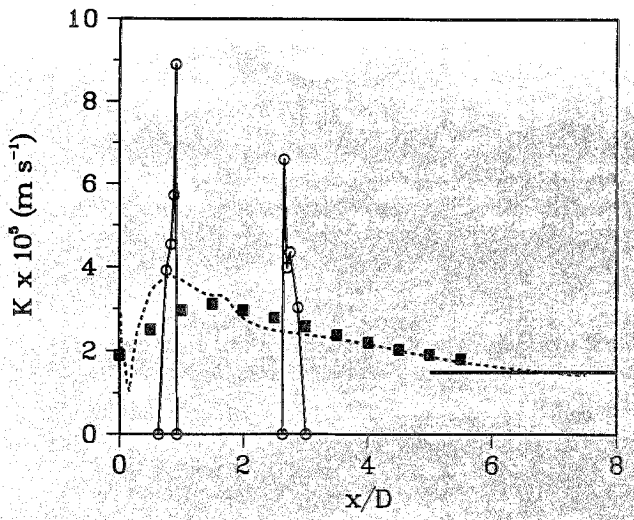

Figure 6 — Mass transfer coefficient at a sudden expansion; d_{in} = 20.0 mm; d_{out} = 40.0 mm; v_{in} = 1.71 m/s; v_{out} = 0.42 m/s; $Re_{out} = 2.1 \times 10^4$; σ_m = 0.9–1.7; Sc = 1460

- - - - $k - \epsilon$, LRN predictions, mass transfer to all of the surface (Nešić et al., 1991)

o $k - \epsilon$, LRN predictions, mass transfer to two 5 mm long patches, (present study)

■ Sydberger and Lotz (1982) measurements

— Berger and Hau (1977) straight pipe correlation.

are sometimes removed selectively by the effects of fluid turbulence or particle impingement under conditions of disturbed flow. The exposed areas corrode at a high rate governed by the local rate of mass transfer of for example dissolved oxygen to the wall. The results in Figure 6 show that this effect can be quantified. As might be expected the rates of local mass transfer to the small active areas decrease rapidly in the direction of the flow at the wall. The flow and the direction of the development and thickening of the mass transfer boundary layer is upstream in the recirculating zone prior to the reattachment point and downstream after the reattachment point.

Conclusions

For engineering flows the WF approach may be considered satisfactory for hydrodynamic calculations given the increase in computing time and storage required by the LRN model. However for mass transfer studies the LRN model permits the determination of the concentration field of the transported species under consideration deep within the viscous sublayer permitting the calculation of local mass transfer coefficients. For mass transfer calculations the LRN treatment is clearly more desirable than the WF based correlation route previously taken (Nešić and Postlethwaite, 1991) since it offers a general solution which does not require a geometry specific correlation between local near wall turbulence and local wall mass transfer coefficients.

Acknowledgement

The support of this research by the Natural Sciences and Engineering Research Council of Canada is gratefully acknowledged.

Nomenclature

$C_\mu, C_{\epsilon 1}, C_{\epsilon 2}$ = constants in $k - \epsilon$ model of turbulence

D = pipe diameter, m

D_{eff} = effective diffusivity, m^2/s

E = constant in the logarithmic wall function

k = kinetic energy of turbulence, m^2/s^2

K = mass transfer coefficient, m/s

P = pressure, N/m^2

r = radial coordinate, m

R = pipe radius, m

Re = Reynolds number, $Re = uD/\nu$

Sc = Schmidt number, $Sc = \nu/D$

$\bar{u}, \bar{v}, \bar{w}$ = components of the fluctuation velocity vector, m/s

U = axial component of mean velocity vector, m/s

U^+ = nondimensional velocity

U_τ = friction velocity, m/s

V = radial component of mean velocity vector, m/s

x = axial coordinate, m

x_r = reattachment length, m

y^+ = nondimensional distance from the wall

Greek letters

δ = Kronecker's delta

ϵ = dissipation rate of kinetic energy of turbulence, m^2/s^3

κ = constant in the logarithmic wall function

ν = kinematic viscosity, m^2/s

ρ = density, kg/m^3

σ_m = turbulent Prandtl–Schmidt number

τ_w = wall tangential shear stress, $kg/m \cdot s^2$

Subscripts

c = refers to point c close to the wall

eff = refers to effective value (molecular + turbulent)

i, j = refer to coordinate directions x, r

k = refers to kinetic energy of turbulence

t = refers to turbulent value

w = refers to a wall value

ϵ = refers to dissipation of kinetic energy of turbulence

References

Berger, F. P. and K.-F. F.-L. Hau, "Mass Transfer in Turbulent Pipe Flow Measured by the Electrochemical Method", Int. J. Heat Mass Transfer **20**, 1185–1194 (1977).

Durrett, R. P., W. H. Stevenson and H. D. Thompson, "Radial and Axial Turbulent Flow Measurements with an LDA in an Axisymmetric Sudden Expansion Air Flow", ASME, J. Fluids Eng. **110**, 367–372 (1988).

Hinze, J. O., "Turbulence", 2nd ed., McGraw-Hill, New York (1975), pp. 23–26.

Kays, W. M. and M. E. Crawford, "Convective Heat and Mass Transfer", McGraw Hill, New York (1980), p. 225–229.

Lam, C. K. G. and K. Bremhost, "A Modified Form of the $k - \epsilon$ Model for Predicting Wall Turbulence", ASME J. Fluids Eng. **103**, 456–460 (1981).

Launder, B. E. and D. B. Spalding, "The Numerical Computation of Turbulent Flows", Comp. Methods Appl. Mech. Eng. **3**, 269–289 (1974).

Nagano, Y. and M. Tagawa, "An Improved $k - \epsilon$ Model for Boundary Layer Flows", J. Fluids Eng. **112**, 33–39 (1990).

Nešić, S., "Computation of Localized Erosion–Corrosion in Disturbed Two-Phase Flow", Ph.D. thesis, University of Saskatchewan, Saskatoon, SK (1991).

Nešić, S. and J. Postlethwaite, "Hydrodynamics of Disturbed Flow and Erosion–Corrosion. Part I. Single-phase Flow Study", Can. J. Chem. Eng. **69**, 698–703 (1991).

Nešić, S., J. Postlethwaite and D. J. Bergstrom, "Calculation of Wall Mass Transfer Rates in Separated Aqueous Flow Using Low Reynolds Number $k - \epsilon$ Model", Int. J. Heat Mass Transfer **35**, 1977–1985 (1992).

Patankar, S. V. and D. B. Spalding, "A Calculation Procedure for Heat, Mass and Momentum Transfer in Three-Dimensional Parabolic Flows", Int. J. Heat Mass Transfer **15**, 1787–1806 (1972).

Patel, V. C., W. Rodi and G. Scheurer, "Turbulence Models for Near-Wall and Low Reynolds Number Flows", AIAA J. **23**, 1308–1319 (1985).

Stieglmeier, M., C. Tropea, N. Weiser and W. Nitsche, "Experimental Investigation of the Flow Through Axisymmetric Expansions", ASME, J. Fluids Eng. **111**, 464–471 (1989).

Sydberger, T. and U. Lotz, "Relation between Mass Transfer and Corrosion in a Turbulent Pipe Flow", J. Electrochem. Soc. **129**, 276–283 (1982).

Yap, C. R., "Turbulent Heat and Momentum Transfer in Recirculating and Impinging Flows", Ph.D. thesis, Univ. of Manchester, Manchester, U.K. (1987).

Zeisel, H. and F. Durst, "Computations of Erosion–Corrosion Processes in Separated Two-Phase Flows", NACE Corrosion/90 Conf., paper No. 29, NACE, Houston, TX, April 23–27 (1990).

Manuscript received February 14, 1992; revised manuscript received June 26, 1992; accepted for publication July 26, 1992.